Heliyon 9 (2023) e15979

Contents lists available at ScienceDirect

Heliyon

journal homepage: www.cell.com/heliyon

Research article

# Adsorption behaviors and influencing factors of antibiotic norfloxacin on natural kaolinite-humic composite colloids in aquatic environment

Dengmiao Cheng [a], Jianyu Chen [a], Jing Wang [c], Xinhui Liu [b,c,*]

[a] Research Center for Eco-Environmental Engineering, Dongguan University of Technology, Dongguan, 523808, PR China
[b] Research and Development Center for Watershed Environmental Eco-Engineering, Beijing Normal University, Zhuhai, 519087, PR China
[c] State Key Laboratory of Water Environment Simulation, School of Environment, Beijing Normal University, Beijing, 100875, PR China

ARTICLE INFO

*Keywords:*
Norfloxacin
Adsorption
Composite colloids
Kaolinite
Humic and fulvic acids

ABSTRACT

Particles are ubiquitous and abundant in natural waters and play a crucial role in the fate and bioavailability of organic pollution. In the present study, natural mineral (kaolinites, KL), organic (humic/fulvic acid, HA/FA) and their composite particles were further separated into particles fractions (PFs, >1 μm) and colloidal fractions (CFs, 1 kDa-1 μm) by cross-flow ultrafiltration (CFUF). This research demonstrated the role of kaolinite-humic composite colloids on the adsorption of fluoroquinolone norfloxacin (NOR). The Freundlich model satisfactory described adsorption curves, showing strong affinity of NOR to CFs, with sorption capacity ($K_F$) between 8975.50 and 16638.13 for NOR. The adsorption capacities of NOR decreased with the particle size increasing from CFs to PFs. In addition, composite CFs showed excellent adsorption capacity, which was mainly attributed to the larger specific surface area of composite CFs and electronegativity and numerous oxygen-containing functional groups on the surfaces of the complexes, and electrostatic attraction, hydrogen bond and cation exchange could dominate the NOR adsorption onto the composite CFs. The best pH value under adsorption condition of composite CFs varied from weakly acidic to neutral with the increase of load amount of humic and fulvic acids on the surface of inorganic particles. The adsorption decreased with higher cation strength, larger cation radius and higher cation valence, which depended on the surface charge of colloids and the molecular shape of NOR. These results provided insight into the interfacial behaviors of NOR on the surfaces of natural colloids and promoted the understanding of the migration and transport of antibiotics in environmental systems.

## 1. Introduction

Antibiotics are widely used in the human and animal health for disease treatment and prevention and even in the livestock and poultry industries as growth promoters [1,2]. Excessive usage and incomplete waste disposal lead to the release of antibiotics into the aquatic environment by various pathways [3–5]. If the bacterial community continually exposes to the antibiotics or its active metabolites in aquatic environment, it will cause the emergence of the antibiotic-resistant bacteria and accelerate the generation of antibiotic resistance genes (ARGs) under the pressure low levels of antibiotics, which could lead to humans be threatened by infections

* Corresponding author.Advanced Institute of Natural Science Beijing Normal University Zhuhai, 519087, PR China.
*E-mail address:* xhliu@bnu.edu.cn (X. Liu).

https://doi.org/10.1016/j.heliyon.2023.e15979
Received 17 February 2023; Received in revised form 27 April 2023; Accepted 28 April 2023
Available online 1 May 2023

caused by exposure to bacteria [6,7]. In recent decades, most of antibiotics are frequently detected in aquatic environment [1]. Contamination with fluoroquinolones (FQs), the third-generation of spectral antimicrobial quinolone antibiotics, has been widely reported in different aquatic matrices including surface water, groundwater, sewage, or sediment samples, and the levels of FQs in water environment ranged from fractions of μg $L^{-1}$ to hundreds of mg $L^{-1}$ [8,9]. So, researching FQs pollution has become gradually a focus in aquatic environment.

Many studies have confirmed that antibiotics were not readily biodegradable, and therefore the residues can readily be found in different aquatic environments due to their adsorption properties [10]. Therefore, it is essential to elucidate antibiotics interaction with diffusing small particles (i.e. colloid and nanoparticle) to understand their transport, transformation and fate in natural waters [11–13]. The mean concentrations of antibiotics ranged between 297 and 3073 ng $g^{-1}$ in the colloid particles that accounted for 4.7–49.8% of all antibiotics, suggesting that natural colloids (NCs) can act as potential adsorption sites for antibiotics [14]. Although the adsorption of antibiotics to environmental substrates such as coarse and sediment have been studied [15,16], but few studies have focused on the adsorption behaviors of antibiotics on NCs.

NCs may reach a maximum of $10^8$ particles per liter, and predominantly consist of inorganic and organic compositions in aquatic environments [17]. Humic substances, including humic acids (HA) and fulvic acids (FA), are the most active multiphase organic components in natural water, soils and sediments with a complex chemical structure including carboxyl, phenolic, ketone and other active groups, which play an important role in controlling the geochemistry behavior of organic matters [18]. In addition, as the most abundant inorganic mineral in aquatic systems, kaolinite (KL) contains large voids, present high specific surface areas and high ion exchange capacities, which composed of interlinked silicon-oxygen tetrahedra and aluminum-oxygen octahedral [18]. The inorganic mineral and natural humic substances form intimate structures lead to a more complicated structure in which small NCs. It is widely accepted that the adsorption of organic material masks the properties of the mineral particles in surface water. NCs contain a large number of functional groups and have significant difference in chemical compositions. For instance, the importance of colloids is often ascribed to an increase in specific surface area with decreasing size resulting in the exposure of a greater number of functional groups at the solid-aqueous interface and thus a greater uptake of trace pollutants [19]. The adsorption of antibiotics on NCs is generally attributed to the special properties and affinity of NCs to antibiotics [20–23]. The fate of antibiotics in aquatic environment has been controlled by the physicochemical properties of NCs (such as size, zeta-potential, specific surface area, organic carbon content) [23]. In the colloidal size range, many studies have focused on the adsorption of antibiotics onto different types of inorganic minerals, such as kaolinite, montmorillonite and ferrihydrite [24,25]. Different types of humic substances, such as HA and FA, could alter many of the physical and chemical properties of minerals, including their rate of dissolution and the physical stability of colloidal particles [26]. Hence, it is necessary to systematically study the behavior of antibiotics at the interfaces of HA/FA and mineral composite colloids with different properties rather than focus on a single model interface.

The adsorption behavior of antibiotics in the environment mainly depends on the structures and physicochemical properties of antibiotics, and related to the physicochemical characteristics of the surrounding environment, such as organic matters, metal elements and pH [23,27]. The most antibiotics are amphoteric molecules that exist in complex speciation behaviors under various pH, their behaviors are highly pH dependent [28,29]. In aquatic environment, the most NCs were negatively charged. Some others were amphoteric NCs that depended on pH, which the surface sites of particles are peculiarly prone to undergo proton exchange [30]. The dissociation degree and solubility of functional groups and the surface charges on NCs surface could be changed in the pH range, which had effects on the amount of adsorption sites on NCs. The adsorption of antibiotics on NCs were related to the surface properties of NCs and the molecular form of antibiotics under various pH, the adsorption mechanism of antibiotics on NCs was described the role of electrostatic attraction, hydrogen bond and cation exchange [31–34]. Antibiotics adsorption depended on atomic radius and valence of metal cations, metal cations competed with antibiotics for positively charged groups of particles and may enhanced the adsorption by bridging bonds [35,36].

In the current studies, the NCs have been found that have strong interactions with antibiotics, we hypothesized that the absorption characteristics of antibiotics on various colloid particles would mainly depend on the surface physicochemical properties of particles [37,38]. In this study, different composite mineral-humic colloids were prepared, and norfloxacin (NOR) was selected as target pollutant owing to its widely used human and livestock treatment, which has been found in a wide range of environmental samples [8, 39]. The primary objectives of this study were to discern the role of natural composite colloids with kaolinites (KL) and humic/fulvic acid (HA/FA) during the adsorption of NOR. In addition, the effects of the environmental pH, strength and species of cation were examined during the adsorption of NOR on composite colloids. This study is important for understanding the behaviour and role of natural colloids in environmental systems, and further expanded the insight into the interfacial behaviors of antibiotics on the surfaces of natural suspended particulate matter.

## 2. Materials and methods

### 2.1. Chemicals and materials

NOR was acquired from Dr. Ehrenstorfer (Augsburg, Germany). Methanol and acetonitrile (HPLC grade) were obtained from Fisher Science Company. Kaolinite and humic acid (HA) were purchased from Sigma-Aldrich (Shanghai, China). Fulvic acid (FA) was purchased from Fluka (Buchs, Switzerland). Unless otherwise indicated, the other chemicals used in this study were of analytical grade. Ultrapure water was obtained from a Milli-Q Advantage A10 system (Millipore, USA). The stock solution (500 mg $L^{-1}$) of NOR was prepared in methanol and kept at −20 °C.

**Table 1**
The physicochemical properties of the particles including particulate fractions (PFs) and colloidal fractions (CFs).

| Particles type | Abbr. | TOC (%)[a] | Size distribution (%) | $f_{HS}$ (%)[b] | Specific surface area (m2 $g^{-1}$) | Pore volume ($cm^3$ $g^{-1}$) | Particles type | Abbr. | TOC (%)[a] | Size | $f_{HS}$ (%)[b] | Specific surface Area (m2 $g^{-1}$) | Pore volume ($cm^3$ $g^{-1}$) |
|---|---|---|---|---|---|---|---|---|---|---|---|---|---|
| KL particulate fractions | $PF_{KL}$ | 0 | 58.54 (1–10 μm) 38.90 (10–50 μm) 2.56 (50–100 μm) | 0.00 | 10.22 | 0.106 | KL colloidal fractions | $CF_{KL}$ | 0 | 1 kDa-1μm | 0.00 | 16.96 | 0.018 |
| | | | | | | | HA colloidal fractions | $CF_{HA}$ | 51.13 | 1 kDa-1μm | 100.00 | 28.10 | 0.025 |
| | | | | | | | FA colloidal fractions | $CF_{FA}$ | 45.33 | 1 kDa-1μm | 100.00 | 26.65 | 0.017 |
| KL-HA particulate fractions | $PF_{KL-HA}$-1 | 0.193 | 55.03 (1–10 μm) 42.30 (10–50 μm) 2.57 (50–100 μm) | 0.43 | 12.13 | 0.118 | KL-HA colloidal fractions | $CF_{KL-HA}$-1 | 2.833 | 1 kDa-1μm | 5.67 | 20.16 | 0.029 |
| | $PF_{KL-HA}$-2 | 0.336 | 57.49 (1–10 μm) 38.83 (10–50 μm) 3.25 (50–100 μm) | 0.76 | 14.72 | 0.137 | | $CF_{KL-HA}$-2 | 4.604 | 1 kDa-1μm | 9.79 | 22.00 | 0.037 |
| | $PF_{KL-HA}$-3 | 1.039 | 56.94 (1–10 μm) 39.26 (10–50 μm) 2.73 (50–100 μm) | 2.21 | 18.83 | 0.186 | | $CF_{KL-HA}$-3 | 6.237 | 1 kDa-1μm | 12.72 | 26.38 | 0.058 |
| KL-FA particulate fractions | $PF_{KL-FA}$-1 | 0.264 | 56.94 (1–10 μm) 38.65 (10–50 μm) 2.67 (50–100 μm) | 0.57 | 12.75 | 0.096 | KL-FA colloidal fractions | $CF_{KL-FA}$-1 | 1.800 | 1 kDa-1μm | 3.91 | 18.73 | 0.021 |
| | $PF_{KL-FA}$-2 | 0.272 | 55.76 (1–10 μm) 40.90 (10–50 μm) 2.29 (50–100 μm) | 0.57 | 12.98 | 0.124 | | $CF_{KL-FA}$-2 | 3.330 | 1 kDa-1μm | 7.35 | 20.14 | 0.029 |
| | $PF_{KL-FA}$-3 | 1.25 | 57.54 (1–10 μm) 38.62 (10–50 μm) 2.97 (50–100 μm) | 2.71 | 13.65 | 0.145 | | $CF_{KL-FA}$-3 | 6.440 | 1 kDa-1μm | 13.56 | 24.01 | 0.035 |

[a] the humus organic carbon accounted for mass percentage of composite particles.
[b] the humic substances accounted for mass percentage of composite particles.

### 2.2. Preparation and characterization of multiple particles

#### 2.2.1. Preparation of particles fractions

As previously reported method with appropriate modification [33], different concentrations of HA/FA solutions (10,000 mL) was mixed with kaolinite (50 g) in ultrapure water medium (solid/liquid ratio = 1:200). The suspensions were intermittently stirred for 2 weeks at 25 °C [40]. Then, the suspensions were passed through the 1 μm filter membrane (Millipore) using suction filtration, and the particulate fractions (PFs) were intercepted on the filter membrane. After being washed with ultrapure water three times, the filter membrane carrying the complex was placed in ultrapure water for ultrasonic dispersion. Finally, the PFs of composite particles loaded with different HA and FA were obtained as follows: $PF_{KL\text{-}HA}$-1, $PF_{KL\text{-}HA}$-2, $PF_{KL\text{-}HA}$-3, $PF_{KL\text{-}FA}$-1, $PF_{KL\text{-}FA}$-2 and $PF_{KL\text{-}FA}$-3 by freeze-drying, and the particle size of these complexes was PFs >1 μm.

#### 2.2.2. Preparation of colloidal fractions

The prefiltered samples were further processed by cross-flow ultrafiltration (CFUF) (0.5 $m^2$ surface area, Millipore Pellicon 2) equipped with 1-kDa PLAC ultrafiltration membrane cassettes. As described in our previous studies [41], the filter operations were carried out in concentration and diafiltration modes, to obtain the corresponding colloidal fractions (CFs) ($CF_{KL\text{-}HA}$-1, $CF_{KL\text{-}HA}$-2, $CF_{KL\text{-}HA}$-3, $CF_{KL\text{-}FA}$-1, $CF_{KL\text{-}FA}$-2 and $CF_{KL\text{-}FA}$-3) on a scale of 1 kDa-1.0 μm. These six different aquatic FCs of complexes were further evaporated using a vacuum rotary evaporator (IKA RV05) below 50 °C to remove much of the water, and then the concentrated solution was freeze-dried into dry CFs. As controls, the particulate fraction ($PF_{KL}$) and colloidal fraction ($CF_{KL}$) of kaolin and the colloidal fractions of HA and FA were $CF_{HA}$ and $CF_{FA}$, respectively, were prepared by the same previous methods.

#### 2.2.3. Characterization

All particles were analyzed for total organic carbon (TOC) content with a TOC analyzer (Shimadzu TOC-L CPN, Japan). Size distributions of PFs were determined by laser particle size analyzer (MicroTrac, S3500, USA). The specific surface areas (SSA) and pore volumes of PFs and CFs were tested using the multiple-point Brunauere-Emmette-Teller (BET) method, with the Autosorb-iQ (Quantachrome Instruments, USA). All these physicochemical properties of the PFs and CFs are summarized in Table 1.

### 2.3. Adsorption experiments

The NOR adsorptions on the various particles were conducted to determine the equilibrium isotherms by batch experiments, which were performed by keeping the 20 mg $L^{-1}$ of PFs or CFs in contact with 20 mL solutions containing different concentrations of NOR (1.0–10.0 mg $L^{-1}$) in 50-mL polypropylene centrifuge tubes. Under optimal conditions, the equilibrium isotherms of NOR were investigated with a mechanically shaking period of 24 h at 150 rpm and 25 ± 1 °C in the dark. Each experiment was repeated three times. The blanks (no particles) at each initial concentration were conducted following the same test procedure. In addition, all the adsorption experiments were carried out under strict dark conditions.

Sorption isotherms were obtained by plotting the sorbed amount $Q_e$ (mg $kg^{-1}$) at equilibrium as a function of equilibrium concentration $C_e$ (mg $L^{-1}$) in solution according to Equation (1) :

$$Q_e = \frac{(C_0 - C_e) \times V}{m} \tag{1}$$

where $C_0$ (mg $L^{-1}$) is the initial NOR concentration, $V$ (L) is the volume of the NOR solution, and $m$ (kg) is the mass of the adsorbent used.

Four isotherm models as Langmuir, Freundlich, Temkin and Dubinin-Radushkevich (D-R) were used for analysis of equilibrium adsorption data according to Equations (2)–(5), respectively:

Langmuir isotherm:

$$\frac{C_e}{Q_e} = \frac{C_e}{Q_{max}} + \frac{1}{K_L Q_{max}} \tag{2}$$

Freundlich isotherm:

$$\mathrm{Ln}\ Q_e = \mathrm{Ln}\ K_F + \frac{1}{n}\mathrm{Ln}\ C_e \tag{3}$$

Temkin isotherm:

$$Q_e = \frac{RT}{b_T}\mathrm{Ln}\ K_T + \frac{RT}{b_T}\mathrm{Ln}\ C_e \tag{4}$$

D-R isotherm:

$$\mathrm{Ln}\ Q_e = \mathrm{Ln}\ Q_{max} - \beta\varepsilon^2 \tag{5}$$

$$\varepsilon = RT\ \mathrm{Ln}\left(1 + \frac{1}{C_e}\right) \tag{6}$$

$$E_a = \frac{1}{\sqrt{2\beta}} \quad (7)$$

where $Q_{max}$ (mg kg$^{-1}$) is the Langmuir maximum capacity, $K_L$ (L mg$^{-1}$) is the Langmuir constant; $K_F$ [(mg kg$^{-1}$)/(mg L$^{-1}$)$^n$] is the Freundlich constant or capacity factor, $n$ is the Freundlich exponent; $K_T$ (L mg$^{-1}$) is the equilibrium binding constant, $b_T$ is the Temkin isotherm constant, $RT/b_T$ (J mol$^{-1}$) is related with adsorption heat; $\beta$ (mol$^2$ kJ$^{-2}$) and $\varepsilon$ (kJ mol$^{-1}$, Equation (6)) are Dubinin-Radushkevich isotherm constants related to the adsorption energy and potential, respectively, $E_a$ is the mean free energy of adsorption (kJ mol$^{-1}$, Equation (7)); $R$ (8.314 J mol$^{-1}$ K$^{-1}$) is the universal gas constant, and $T$ (298.15 K) is the absolute temperature.

To assess the pH effects of the NOR adsorption on CFs, the pH of CFs solution was adjusted from 3 to 11 with 0.1 M HCl or NaOH. Five types cations ($Na^+$, $K^+$, $Mg^{2+}$, $Ca^{2+}$ and $Al^{3+}$) were investigated by using NaCl, KCl, $MgCl_2$, $CaCl_2$ and $AlCl_3$ (1 mM) to assess the cation effects of the NOR adsorption on CFs. In addition, to assess the cation strength effects of the NOR adsorption on CFs, the cation strength of CFs solution was adjusted in the range 0.1–5.0 mM using $CaCl_2$. The other experimental conditions and measurements were the same as described above.

### 2.4. Sample preparation and analysis

Each sample (0.5 mL) was centrifuged and filtered through a 1 kDa ultrafiltration centrifuge tubes (Pall Filtron, USA) at 12000 rpm for 10 min to obtain soluble phases. The concentrations of NOR were analyzed by HPLC using a Thermo Scientific Dionex Ultimate 3000 apparatus equipped with a Waters Symmetry C18 column (4.6 × 250 mm, 5 μm). The column temperature was maintained at 30 °C. The mobile phase was composed of 0.1% (v/v) phosphoric acid in ultrapure water and acetonitrile at a ratio of 83:17 and a flow rate of 1 mL min$^{-1}$. An injection volume of 10 μL was used in all analyses. The detection wavelengths of the NOR was 278 nm, and a good linearity between the peak areas and the NOR concentrations was observed in the ranges of 0.1–10 μg mL$^{-1}$ with $R^2 > 0.999$. The limits of detection (LODs) and quantification (LOQs) for NOR, estimated as the signal-to-noise (S/N) ratios of 3 and 10, were 0.10 μg mL$^{-1}$ and 0.33 μg mL$^{-1}$, respectively.

### 2.5. Quality assurance and statistical analysis

To assess the adsorption of antibiotics on the ultrafiltration centrifuge tubes, the recovery was performed using the standard NOR solutions with different initial concentrations (1.0–10.0 mg L$^{-1}$), which were centrifuged and filtered through the 1 kDa ultrafiltration

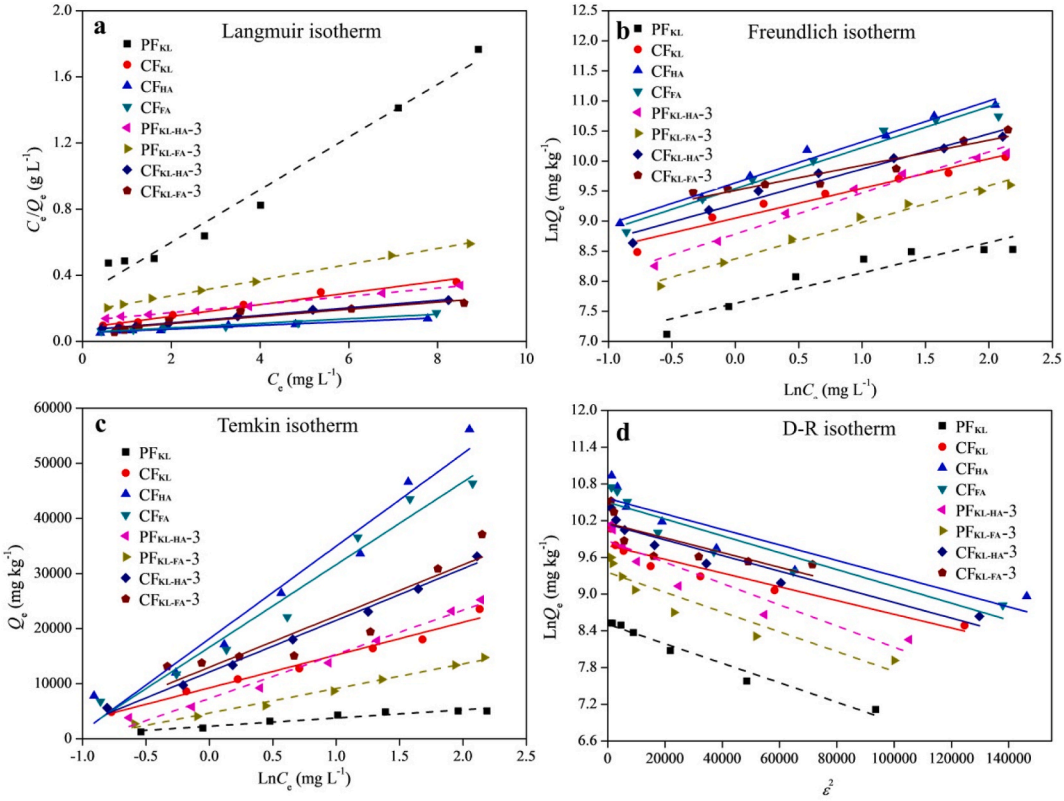


**Fig. 1.** Fittings of NOR adsorption isotherms onto various particles: (a) Langmuir, (b) Freundlich (c) Temkin, and (d) D-R models.

**Table 2**
The parameters of isotherms for NOR adsorption on various particles.

| Particles type | Freundlich model | | | Langmuir model | | | Temkin model | | | D-R model | | | |
|---|---|---|---|---|---|---|---|---|---|---|---|---|---|
| | $K_F$[a] | n | $R^2$ | $Q_{max}$ (mg $g^{-1}$) | $K_L$ (L $mg^{-1}$) | $R^2$ | $b_T$ | $K_T$ (L $mg^{-1}$) | $R^2$ | $Q_{max}$ (mg $g^{-1}$) | $\beta$ ($mol^2$ $kJ^{-2}$) | $E_a$ (kJ $mol^{-1}$) | $R^2$ |
| Particulate fractions (PFs) | | | | | | | | | | | | | |
| $PF_{KL}$ | 2456.06 | 1.969 | 0.818 | 6.42 | 0.58 | 0.945 | 0.206 | 4.675 | 0.982 | 4.95 | 1.589E-05 | 177.412 | 0.969 |
| $PF_{KL-HA}$-1 | 4716.62 | 1.563 | 0.988 | 25.49 | 0.20 | 0.996 | 0.061 | 2.551 | 0.969 | 16.29 | 1.657E-05 | 173.725 | 0.825 |
| $PF_{KL-HA}$-2 | 5364.33 | 1.701 | 0.998 | 26.37 | 0.22 | 0.992 | 0.059 | 2.869 | 0.965 | 16.94 | 1.471E-05 | 184.390 | 0.806 |
| $PF_{KL-HA}$-3 | 7410.54 | 1.462 | 0.979 | 39.79 | 0.21 | 0.999 | 0.038 | 2.491 | 0.982 | 26.08 | 1.736E-05 | 169.714 | 0.859 |
| $PF_{KL-FA}$-1 | 4490.05 | 1.650 | 0.926 | 16.46 | 0.34 | 0.985 | 0.081 | 3.083 | 0.984 | 14.09 | 1.706E-05 | 171.206 | 0.913 |
| $PF_{KL-FA}$-2 | 5609.81 | 1.712 | 0.972 | 21.99 | 0.31 | 0.997 | 0.064 | 3.146 | 0.992 | 17.15 | 1.555E-05 | 179.299 | 0.886 |
| $PF_{KL-FA}$-3 | 4778.48 | 1.645 | 0.980 | 20.98 | 0.26 | 0.999 | 0.069 | 2.857 | 0.988 | 15.40 | 1.616E-05 | 175.896 | 0.863 |
| Colloidal fractions (CFs) | | | | | | | | | | | | | |
| $CF_{KL}$ | 12515.50 | 1.581 | 0.977 | 27.49 | 0.46 | 0.961 | 0.051 | 4.734 | 0.974 | 21.32 | 1.122E-05 | 211.116 | 0.893 |
| $CF_{HA}$ | 16638.13 | 1.468 | 0.980 | 90.71 | 0.21 | 0.989 | 0.018 | 2.947 | 0.953 | 45.02 | 1.264E-05 | 198.896 | 0.800 |
| $CF_{FA}$ | 16234.51 | 1.462 | 0.974 | 70.87 | 0.28 | 0.926 | 0.020 | 3.028 | 0.962 | 43.72 | 1.374E-05 | 190.766 | 0.852 |
| $CF_{KL-HA}$-1 | 9900.24 | 1.923 | 0.956 | 28.87 | 0.51 | 0.946 | 0.047 | 4.509 | 0.969 | 23.34 | 1.189E-05 | 205.037 | 0.902 |
| $CF_{KL-HA}$-2 | 11135.30 | 1.942 | 0.961 | 29.41 | 0.51 | 0.948 | 0.046 | 4.616 | 0.974 | 23.74 | 1.170E-05 | 206.683 | 0.904 |
| $CF_{KL-HA}$-3 | 11668.69 | 1.704 | 0.994 | 43.85 | 0.34 | 0.975 | 0.033 | 3.642 | 0.972 | 30.61 | 1.277E-05 | 197.840 | 0.893 |
| $CF_{KL-FA}$-1 | 9291.89 | 1.946 | 0.986 | 36.97 | 0.30 | 0.984 | 0.038 | 2.908 | 0.973 | 31.95 | 1.879E-05 | 163.140 | 0.794 |
| $CF_{KL-FA}$-2 | 11164.24 | 2.146 | 0.979 | 55.31 | 0.22 | 0.894 | 0.035 | 4.042 | 0.885 | 32.86 | 1.198E-05 | 204.315 | 0.601 |
| $CF_{KL-FA}$-3 | 10372.98 | 2.392 | 0.971 | 44.19 | 0.27 | 0.850 | 0.033 | 3.243 | 0.830 | 31.23 | 1.450E-05 | 185.186 | 0.521 |

[a] $K_F$ [(mg $kg^{-1}$)/(mg $L^{-1})^n$] sorption capacity coefficient from Freundlich model.The parameters of isotherms for NOR adsorption on various particles.

centrifuge tubes at 12000 rpm for 10 min to obtain soluble phases. The recovery rate ($R$) was determined by dividing the concentration of NOR remaining in soluble phases ($C_w$) by the initial concentration of NOR ($C_0$) (*i.e.*, $R = C_w/C_0 \times 100\%$), and the $R$ values were higher, which can reach 91.17–103.48%.

The plotting and fitting of adsorption data were conducted using the OriginPro 8.0 (OriginLab, USA). Pearson's correlation analysis (SPSS software, Windows version 16.0, SPSS Inc.) was performed in order to determine relationships between adsorption capacity and physicochemical properties of PFs and CFs.

## 3. Results and discussion

### 3.1. The NOR adsorption of various particles

#### 3.1.1. The adsorption isotherms of NOR on various particles

As shown in Fig. 1, the adsorption properties of different size fractions of various particles, including the particulate fractions (PFs) and colloidal fraction (CFs), were indicated by the adsorption isotherms of NOR, which were well described by Langmuir, Freundlich, Temkin and Dubinin-Radushkevich (D-R) isotherm models, the fitting parameters of the four isotherm models were listed in Table 2.

As indicated by the correlation coefficient $R^2$, the Langmuir isotherm reasonably fitted the adsorptions of NOR onto PFs, such as $PF_{KL}$, $PF_{KL\text{-}HA}$-3 and $PF_{KL\text{-}FA}$-3 ($R^2 > 0.95$). The Langmuir model assumed that the adsorption was single molecular layer adsorption; the same energy was needed for the interaction occurred on active adsorption sites on homogeneous adsorption surface, and the molecules couldn't interact with each other [42]. This also means that the adsorption of NOR depended on the limited active adsorption sites on coarse particles. This was consistent with the observation that the adsorption isotherm of TC on suspended particulate matter could also be described well by a Langmuir model [43]. The maximum adsorption capacities of NOR on $PF_{KL\text{-}HA}$ ranged from 25.49 to 39.79 mg $g^{-1}$, which was higher than 17$\beta$-estradiol (E2) on KL-HA complexes [33].

However, for CFs, the values of $R^2$ from Freundlich isotherm ($R^2 > 0.97$) are greater than those from Langmuir isotherms ($R^2 > 0.85$), indicating the adsorption process of NOR onto CFs, including $CF_{KL}$, $CF_{HA}$, $CF_{FA}$, $CF_{KL\text{-}HA}$-3 and $CF_{KL\text{-}FA}$-3, was better described by Freundlich isotherm (Table 2). The coefficient $K_F$ of Freundlich model represents the relative adsorption capacity of CFs with NOR, and the value of parameter $n$ is a measure of adsorption intensity, which relates to the heterogeneity of the CFs being examined [44]. When $1 < n < 10$ means that the adsorbate is easily adsorbed [45]. The $n$ values of CFs were in the range from 1.462 to 2.392, indicating the adsorption of NOR onto CFs in Freundlich model were favorable. There were unlimited adsorption sites on the heterogeneous multilayer of CFs that leaded to the high adsorption of NOR. This behavior has previously been reported for the adsorption of tetracycline (TC) and ciprofloxacin (CIP) onto iron oxide minerals, especially for colloidal goethite [46]. Compared with organic colloids ($CF_{HA}$ and $CF_{FA}$), the adsorption isotherms of NOR on inorganic and composite colloids, such as $CF_{KL}$, $CF_{KL\text{-}HA}$-3, and $CF_{KL\text{-}FA}$-3, showed higher $n$ values (ranging from 1.77 to 2.31) (Table 2), indicating that NOR has a greater affinity with inorganic and composite colloids. However, the high affinity (high $n$ value) wasn't analogous to having a high adsorption capacity (high $K_F$ value). The $K_F$ was governed by properties such as the size distribution, the specific surface area and the surface functional groups of particles [47].

To verify the results, Temkin model was also used to fit the adsorption data. Different from the Langmuir and Freundlich models, the Temkin model is supposed that adsorption energy decrease linearly due to the surface coverage, which is more suitable for the chemisorption process that is usually considered to be electrostatic interaction [48]. As shown in Fig. 1c and Table 2, the Temkin isotherm well fitted the adsorption data ($R^2 = 0.83$–$0.99$), indicating that electrostatic interaction was one of mechanisms in the adsorption of NOR onto the minerals and composites. The fitting result also indicated that the adsorption of NOR by the minerals and composites, especially the $PF_s$ ($R^2 > 0.98$), was not uniform single-layer adsorption [49]. Many studies have also shown that the adsorption isotherms of antibiotics on natural and synthetic composites in the nano-size range could be well fitted by Freundlich isotherm [50–52]. Our previous study has shown that the particle size also plays a crucial role in the adsorption behavior except for the physicochemical properties of the particle surface [47].

Moreover, the fitting of D-R model is shown in Fig. 1d, which dedicated to exploring the Gaussian energy distribution onto an uneven surface, and the adsorption type was roughly inferred by a relevant parameter of the mean free energy of adsorption ($E_a$). The values of $E_a$ between 1 and 8 kJ $mol^{-1}$ and between 8 and 16 kJ $mol^{-1}$ corresponds to physical and ion exchange processes, respectively, while the value of $E_a$ greater than 16 kJ $mol^{-1}$ is considered to be chemical adsorption [53]. As shown in Table 2, the values of $E_a$ were all larger than 16 kJ $mol^{-1}$, which indicated that the chemical adsorption mechanism may also play an important role in the adsorption process. However, most of the regression coefficients ($R^2$) of NOR were less than 0.90, it did not describe the adsorption of NOR onto the different size of complexes very well.

#### 3.1.2. Effects of the particle size and specific surface area

As shown in Table 1, with the increase of organic matter content, the particle size and specific surface area of the composite particles also increased. It is generally believed that there is a saturation mechanism for mineral adsorption of organic matter under normal temperature and pressure [54]. Therefore, the humic and fulvic acids on the outer layer of the complex will further interactions with humic and fulvic acids through the electrostatic attraction after it reaches saturation. This relatively loose distribution of humic and fulvic acids on kaolin surface caused a continuous increase in particle size, specific surface area, and empty volume with continuous loading of HA/FA molecules [40]. The relationship of adsorption capacities for different size of particles was as follows: $CF_{HA} > CF_{FA} > CF_{KL} > PF_{KL}$ (Fig. 1). This result revealed that the adsorption capacities of particles decreased with size increasing and increased with specific surface area increasing (Table 1). Pearson correlation analysis also demonstrated that the values of $K_F$ (sorption capacity coefficient) were positively correlated with the specific surface area of PFs ($r = 0.924$, $P < 0.01$) and CFs ($r = 0.835$, $P < 0.01$)

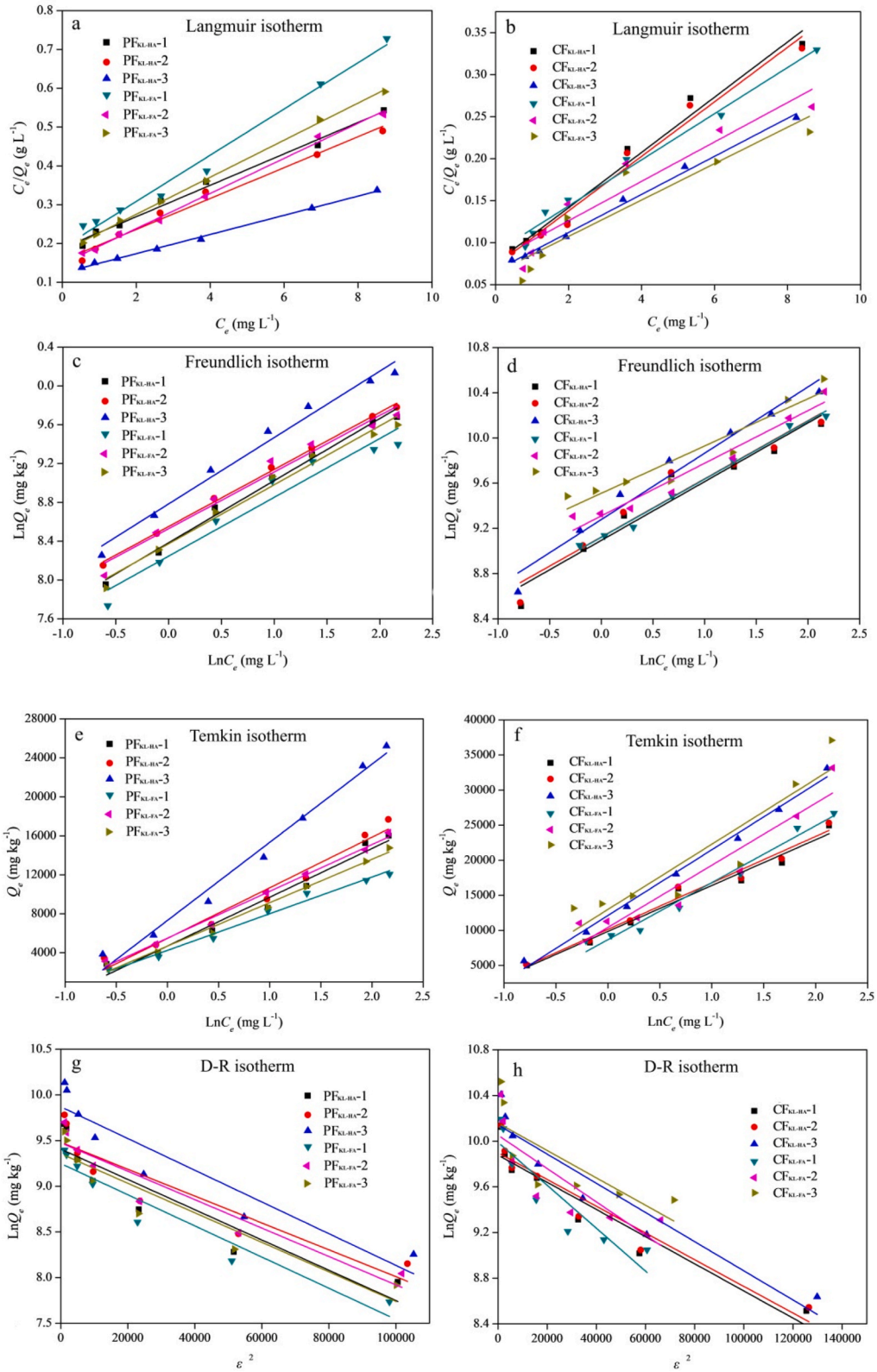


**Fig. 2.** Fittings of NOR adsorption isotherms (Langmuir, Freundlich, Temkin and D-R models) onto composite (a), (c), (e) and (g) $PF_{KL\text{-}HA/FA}$ and (b), (d), (f) and (h) $CF_{KL\text{-}HA/FA}$.

(Tables S1–2). Studies have shown that particle size generally has a strong relationship with adsorption capacity, which is ascribed to the enlarged surface area of particles [55]. The adsorption of some other organic pollutants onto the surface of suspended particulate matter or microplastics also showed the same trend [56,57]. The values of $K_F$ for the NOR adsorption on CFs ranged from 9291.89 to 16638.13 (mg $kg^{-1}$)/(mg $L^{-1}$)$^n$ and much higher than that on PFs. The higher adsorption capacity for $CF_{KL}$ compared to that for $PF_{KL}$, which could be explained that the specific surface area of mineral particles gradually increases with the decrease of particle size, and then smaller particles had higher adsorption sites density.

As "particles state" macromolecules, the organic CFs ($CF_{HA}$ and $CF_{FA}$) had larger specific surface area than $CF_{KL}$, and the higher adsorption capacities of organic CFs were related to the surface functional groups [58]. In addition, the $CF_{HA}$ had stronger adsorption capacities than $CF_{FA}$ related to the larger specific surface area. This result was consistent with a recently published study in which the adsorption efficiencies of nitrapyrin on HA were higher than that on FA [59]. Therefore, the larger specific surface area and smaller particle size enhanced the adsorption sites of particles, and leaded to the stronger adsorption capacities for the particles, which was related to the effectively active adsorption sites of particles.

### 3.1.3. Effects of the humic and fulvic acids

The adsorption process of NOR onto the different size of KL-HA/FA composites were also described by the Langmuir and Freundlich models (Fig. 2a–d), and the Temkin and D-R isotherm models verified related results (Fig. 2e–h). All the fitting parameters of the four isotherms are also listed in Table 2.

The Freundlich model satisfactory described the equilibrium adsorption data of the colloidal fractions of KL, HA/FA and their composites (Fig. 2b), showing strong affinity of NOR to CFs. In addition, Pearson correlation analysis also suggested that the values of $K_F$ were positively correlated with TOC, especially for CFs ($r = 0.876$, $P < 0.01$) (Table S2). The organic CFs had higher adsorption capacities than inorganic CFs, and the $K_F$ values of $CF_{HA}$ (16638.13 (mg $kg^{-1}$)/(mg $L^{-1}$)$^n$) and $CF_{FA}$ (16234.51 (mg $kg^{-1}$)/(mg $L^{-1}$)$^n$) were twice bigger than $CF_{KL}$ (8975.50 (mg $kg^{-1}$)/(mg $L^{-1}$)$^n$). In addition, the values of $K_F$ for adsorption of NOR on composite particles, including $PF_{KL\text{-}HA/FA}$ and $CF_{KL\text{-}HA/FA}$, mostly increased with organic carbon content increasing, which were obviously bigger than that on inorganic particles. Generally, with the increase coating of humic and fulvic acids on inorganic particles, the adsorption capacities of NOR on the composite CFs tended to be similar to the organic CFs. This could be due to a very high degree of surface similarity between them and the effects of humic and fulvic acid layer on composite CPs. Humic and fulvic acids had a crucial role for inorganic particles fate by modifying their surface properties and stability [60–62]. Composite particles displayed a more open arrangement than blank inorganic particles, and the humic and fulvic acids adsorbed on inorganic particles provided additional adsorption sites for NOR [63]. In addition, the extent of dispersion for particles depended on the amount of humic and fulvic acids adsorbed on inorganic particles [64]. The adsorption of humic and fulvic acids played an important role in determining the interparticle forces and stability of CFs and enhanced the mobilisation of CFs. Thus, according to the adsorption equilibrium constants (Table 2), the adsorption capacities of NOR on composite particles were higher than that of NOR on inorganic particles, which were attributed to the higher dispersion and mobilisation of composite particles that could enhance the frequency of collisions and the efficiency of contacts.

As shown in Table 1, the adsorption capacities of composite CFs (11668.69 and 10372.98 (mg $kg^{-1}$)/(mg $L^{-1}$)$^n$ for $K_F$ of $CF_{KL\text{-}HA}$-3 and $CF_{KL\text{-}FA}$-3, respectively) couldn't be equal to that of organic CFs (16638.13 and 16234.51 (mg $kg^{-1}$)/(mg $L^{-1}$)$^n$ for $K_F$ of $CF_{HA}$ and $CF_{FA}$, respectively) when the humic and fulvic acid concentrations of composite CFs reached saturation. This result was explained that the characteristics of humic and fulvic acids such as molecular weight, functional group compositions and hydrophobicity would be corresponding changes during the synthesis of composite CFs [65]. With the continuous adsorption of humic and fulvic acids on inorganic particles, the composite particles had high adsorption capacities and became important factor effecting the NOR adsorption behavior [63,66]. At low levels, the humic and fulvic acids could compete with NOR for the adsorption sites on inorganic particles. However, with the increase of content of humic and fulvic acids, multilayered structures of humic and fulvic acids were formed on inorganic particle surfaces, and the polar functional groups was accumulated on the surface layer of inorganic particles, so the adsorption of ionic compounds (such as NOR) increased with humic and fulvic acids content increased [67].

However, with the increase of total organic carbon (TOC) content (Table 1), the adsorption capacities of Kaolinite-FA composite colloids ($CF_{KL\text{-}FA}$) did not rise but decreased significantly (Table 2). This is beneficial for two main reasons. First, HA has stronger adsorption on inorganic mineral particles than FA and is more difficult to be desorbed than FA [68]. Secondly, due to the smaller molecular weight of FA than HA, the stronger competitive sorption of FA results in reduced NOR sorption on the surface of $CF_{KL\text{-}FA}$ [69]. In addition, TOC dose not account for all of the humic and fulvic acid contents, and the humic and fulvic acids had different effects on the adsorption capacities of composite particles due to their different characteristics and the different adsorption mechanisms of humic substances on various inorganic particles [70]. The effects of humic and fulvic acids on the solubility of NOR were related to their own size, polarity, and molecular configuration [71]. This is an interesting and complex issue that needed to clarify the specific reasons in our further studies.

## 3.2. Effects of the pH

As an amphoteric compound, the NOR has multiple ionizable functional groups ($pK_{a1}$, 6.23; $pK_{a2}$, 8.55), which exists predominantly as zwitterions in aquatic environment [72]. As shown in Fig. 3a. NOR should be underwent protonation and deprotonation reactions, and presented different ionic species depending on the pH of solution in which NOR was dissolved [73,74]. The molecular form of NOR was $NOR^+$ when pH was below its $pK_{a1}$, $NOR^\pm$ when $pK_{a1} < pH < pK_{a2}$, and $NOR^-$ when $pH > pK_{a2}$. In aquatic environment, most CFs is negatively charged that depends on the pH of the solution [75]. The surface charges of natural CFs were

charged by proton exchange with solution [30]. The NOR adsorption on CFs were related to the surface charges of CFs and the molecular form of NOR. Therefore, the effect of pH on the adsorption of NOR onto various CFs was studied in a range from 3 to 11.

### 3.2.1. On kaolinite CFs

As shown in Fig. 3b, the adsorption capacity of NOR on $CF_{KL}$ was relatively high when the pH is 7. Adsorption capacity ($K_F$) of NOR on $CF_{KL}$ was increased from 7828.60 to 9874.39 when the pH values was raised from 3 to 7. Conversely, increasing the pH from 9 to 11 reduces the adsorption capacity ($K_F$) of NOR on $CF_{KL}$ from 9682.58 to 8332.20. Kaolinite was a 1:1 dioctahedral aluminosilicate with the negative surface charges, and the charges of edge sites could be either positive or negative, effectively depended on the pH. The point of zero charge pH ($pH_{PZC}$) of kaolinite was about 2.8 [76]. The surfaces of $CF_{KL}$ were negatively charged above the PZC and positively below that, because of the specific adsorption of charge-determining $H^+$ and $OH^-$ ions. When pH < PZC, the electrostatic repulsion was operated to be predominant reaction when the NOR and kaolinite ultrafine particles were both positively charged [77, 78]. With pH increasing, the surface of kaolinite was negatively charged at pH > 2.8. Consequently, $CF_{KL}$ had a strong electrostatic attraction to NOR since the surface of $CF_{KL}$ had more negative charges at high pH NOR primary existent forms were $NOR^+$ or $NOR^{\pm}$ in the water with a pH range of 3–7. Therefore, negatively charged $CF_{KL}$ could easily adsorb positively charged or neutral NOR. When pH > 7, the species of NOR gradually became neutral ($NOR^{\pm}$) or negative charged ($NOR^-$) through deprotonation with the increase of the pH (Fig. 3a), and the electrostatic repulsion was the predominant reaction to be operated. The decrease of the adsorption of NOR on kaolinite CFs showed that the cation was an important factor for NOR adsorption when the dominant dissolved NOR was the zwitterions ($NOR^{\pm}$). The $NOR^{\pm}$ interacted with the surface sites of $CF_{KL}$ by surface complexation mechanism. According to the structure of kaolinite, the adsorption reaction could mainly occur at the negatively charged surface sites. The ionic strength and electrolyte types were fundamental factors for the adsorption of NOR on kaolinite CFs. The NOR adsorption on kaolinite CFs could depended on the hydration of aluminum oxide surface and the hydrogen bonding of water to the silanol groups of kaolinite, which demonstrated that NOR adsorption mainly depended on ion exchange of cations species and complexation of zwitterions species.

### 3.2.2. On HA/FA and composite CFs

As shown in Fig. 3b, the adsorptions of NOR on $CF_{HA}$ and $CF_{FA}$ were highest at around pH 5.0 and lower with either increased or

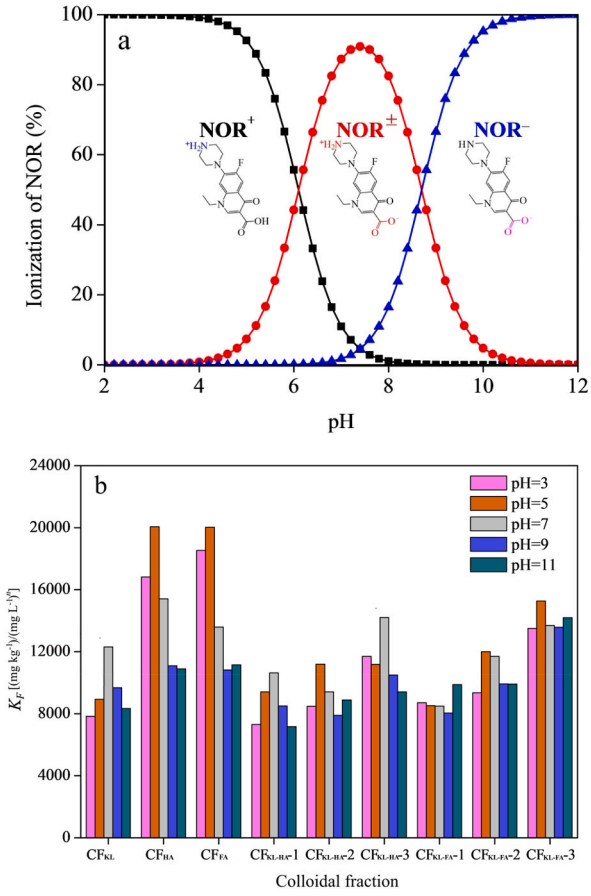


**Fig. 3.** (a) Distribution of NOR molecules at different pH values. (b) Effects of pH on the adsorption of NOR onto various CFs. (adsorption conditions: contact time = 24 h, and temperature = 25 ± 1 °C, in the dark).

decreased in pH. It is well known that organic humus CFs generally were negatively charged that was related to $H^+$ dissociation of numerous oxygen-containing functional groups, such as hydroxyl and carboxyl groups [79]. The cationic and zwitterionic species were predominant forms of NOR, which could be adsorbed on deprotonated sites of $CF_{HA}$ and $CF_{FA}$ through cation exchange or hydrogen bond [80]. When the pH was lower, the predominant form of NOR was cation and the $CF_{HA}$ and $CF_{FA}$ were negatively charged by $H^+$ dissociation. Such adsorption of NOR occurred mainly through the electrostatic adsorption. Additionally, the low pH was conducive to form the hydrogen bond between the carboxyl, amino groups of NOR and the hydroxyl, phenolic, amino of $CF_{HA}$ and $CF_{FA}$ surface, which also could enhance the adsorption of NOR on humic substances CFs surface [81]. Therefore, pH has the greatest effect on the chemical structure and apparent molecular weight of humic and fulvic acids as well as the surface properties and the active adsorption sites of $CF_{HA}$ and $CF_{FA}$.

NOR adsorption onto composite CFs ($CF_{KL\text{-}HA}$ and $CF_{KL\text{-}FA}$) showed a strong pH-dependence in studied pH range (Fig. 3b). At neutral and acidic conditions, the HA/FA coating significantly increased the NOR adsorption with a maximal sorption around pH 5–7, and a greater adsorption increase was observed at the higher humic concentration. At alkaline condition, the adsorption of NOR was slightly enhanced in the humic coating.

The values of $K_F$ tended to the peak shape, especially for $CF_{KL\text{-}HA}$-1 and $CF_{KL\text{-}FA}$-2 that were highest at around pH 7.0 and 5.0, respectively. For the other four treatments ($CF_{KL\text{-}HA}$-2, $CF_{KL\text{-}HA}$-3, $CF_{KL\text{-}FA}$-1 and $CF_{KL\text{-}FA}$-3), there was no obvious regularity of $K_F$ with the increase of pH, and the $K_F$ peaked at pH around 5.0, 5.0, 7.0 and 11.0 for the $CF_{KL\text{-}HA}$-2, $CF_{KL\text{-}FA}$-3, $CF_{KL\text{-}HA}$-3 and $CF_{KL\text{-}FA}$-1, respectively. With lower organic matter content, the effect of pH on the composite CFs was similar to the inorganic CFs. This result mainly depended on the surface properties of the composite CFs with lower organic matter content that were similar to the inorganic CFs. However, with high humic content, the surface properties of composite CFs were similar to that of the organic CFs, and the influence of pH on the surface characteristics of the composite CFs was attributed to the influence of pH on the surface organic components of them. Therefore, with the increase of organic matter content, the optimal pH of NOR adsorption on the composite CFs changed from weakly alkaline to weakly acidic. Humic and fulvic acids contained many acidic functional groups and the humic coating on mineral particles could produce a surface charge on composite CFs, which could influence the morphology of inorganic particles by modifying the surface charges [62].

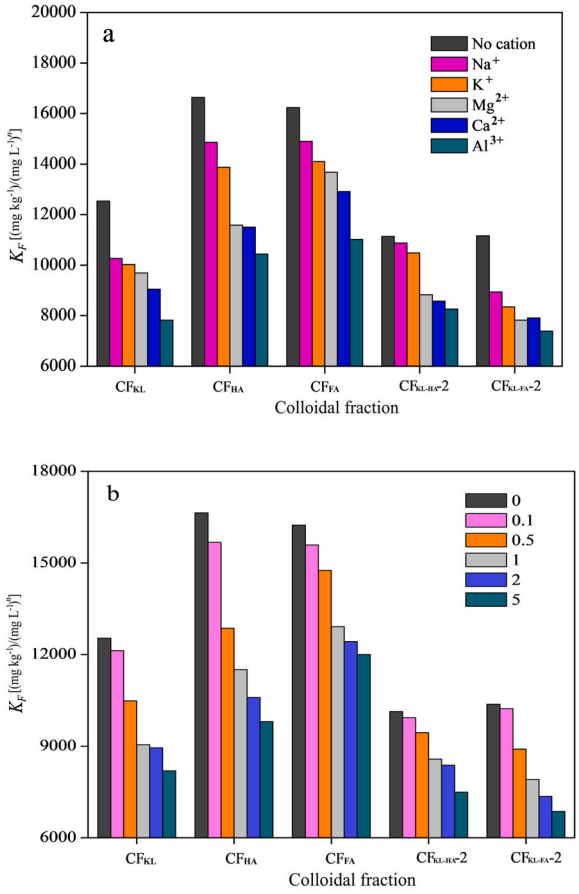


**Fig. 4.** Effects of (a) species and (b) strength of cation onto the adsorption of NOR on various CFs. (adsorption conditions: pH = 7, contact time = 24 h, and temperature = 25 ± 1 °C, in the dark).

### 3.3. Effects of ionic strength and cation species

There are various cations in the aqueous environment, and the influence of different types of cations on the adsorption behavior of NOR on CFs is shown in Fig. 4a. In the presence of different cations, the adsorption capacities of NOR on CFs were changed as follows: $Na^+ > K^+ > Ca^{2+} > Mg^{2+} > Al^{3+}$. Due to the high positive charge of high-valence cation, the ability to compete for the negative adsorption sites on the surface of CFs was stronger at the same cation concentrations, which led to the decrease of NOR adsorption with the increase of cation valence state [82,83]. As monovalent metal ions, $Na^+$ and $K^+$ can compete with $NOR^+$ and inhibit the adsorption behaviors of NOR on CFs. For polyvalent metal ions such as $Mg^{2+}$, $Ca^{2+}$ and $Al^{3+}$, the adsorption of NOR were weakened by competition with cationic NOR. Meanwhile, many studies have also confirmed that these metal ions can promote the adsorption of antibiotics through the bridge bond between antibiotics and sorbent [84,85]. Furthermore, in contrast to the monovalent $Na^+$, the divalent $Ca^{2+}$ led to greater electronic screening effect, and thus has stronger inhibition effect on NOR adsorption by CFs. It's the same with the trivalent $Al^{3+}$. It might be due to the fact that $Ca^{2+}$ and $Al^{3+}$ had bigger hydrated radius and occupied more adsorption sites than that of $Na^+$, and thus they were more capable to inhibit the adsorption of NOR [86].

The influence of ionic strength on the adsorption of NOR in various CFs was investigated at various $CaCl_2$ concentrations. As shown in Fig. 4b, with the addition of $Ca^{2+}$ (0.1–5.0 mM), the values of $K_F$ for adsorption of NOR on the composite colloids decreased with the increase of ionic strength. The declined of NOR uptake would be owing to the competitive effects between NOR cation molecule and the $Ca^{2+}$ ions during the adsorption process. The increasing of ionic concentrations decreased the active sites of the adsorbent, which confirmed the existence of electrostatic interactions between NOR and CFs [73]. In summary, the ionic strength strongly affected the NOR adsorption capacity onto CFs.

## 4. Conclusions

This study investigated the adsorption behaviors and affecting factors of NOR by different size of kaolinite-humic/fulvic acid composites, including particles fractions (PFs, >1 μm) and colloidal fractions (CFs, 1 kDa-1 μm) in aqueous solutions. The adsorption isotherms of NOR on PFs and CFs much more followed the Langmuir and Freundlich models, respectively. The adsorption of NOR was favored by the composite CFs. This result mainly attributed to two aspects: (1) The larger specific surface area and smaller particle size enhanced the adsorption sites of particles, and leaded to the stronger adsorption capacities for the composite CFs; (2) The presence of numerous oxygen-containing functional groups on the surfaces of the composite CFs, which facilitated the electrostatic attraction and generation of cation exchange or hydrogen bonds between the CFs and NOR. In addition, the environmental pH, strength and species of cation had great effect to the adsorption of NOR on composite colloids. These findings have significant implications for understanding the importance of natural colloid and its effect on the fate, migration, and bioavailability of antibiotics, which may provide new conception for the ecological assessment of hydrophilic contaminants in the aquatic environments.

## Author contribution statement

Dengmiao Cheng: Conceived and designed the experiments; Analyzed and interpreted the data; Wrote the paper. Jianyu Chen: Analyzed and interpreted the data. Jing Wang: Performed the experiments. Xinhui Liu: Conceived and designed the experiments; Contributed reagents, materials, analysis tools or data.

## Data availability statement

Data will be made available on request.

## Additional information

Supplementary content related to this article has been published online at [URL].

## Funding statement

This work was financially supported by the Basic and Applied Basic Research Foundation of Guangdong Province, China (2022A1515010751), the Natural Science Foundation of China (31772395 and 21677013), and the Academician Workstation Project of Dongguan (DGYSZ-2018-06).

## Declaration of competing interest

The authors declare that they have no known competing financial interests or personal relationships that could have appeared to influence the work reported in this paper.

## Appendix A. Supplementary data

Supplementary data to this article can be found online at https://doi.org/10.1016/j.heliyon.2023.e15979.

## References


[1] P. Kovalakova, L. Cizmas, T.J. McDonald, B. Marsalek, M. Feng, V.K. Sharma, Occurrence and toxicity of antibiotics in the aquatic environment: a review, Chemosphere 251 (2020), 126351, https://doi.org/10.1016/j.chemosphere.2020.126351.

[2] K. Kümmerer, Antibiotics in the aquatic environment – a review – Part I, Chemosphere 75 (4) (2009) 417–434, https://doi.org/10.1016/j.chemosphere.2008.11.086.

[3] W. Xu, G. Zhang, X. Li, S. Zou, P. Li, Z. Hu, J. Li, Occurrence and elimination of antibiotics at four sewage treatment plants in the Pearl River Delta (PRD), South China, Water Res. 41 (19) (2007) 4526–4534, https://doi.org/10.1016/j.watres.2007.06.023.

[4] D. A, X. Zhang, Y. Dai, C. Chen, Y. Yang, Occurrence and removal of quinolone, tetracycline, and macrolide antibiotics from urban wastewater in constructed wetlands, J. Clean. Prod. 252 (2020), 119677, https://doi.org/10.1016/j.jclepro.2019.119677.

[5] F. Li, L. Chen, W. Chen, Y. Bao, Y. Zheng, B. Huang, Q. Mu, D. Wen, C. Feng, Antibiotics in coastal water and sediments of the East China Sea: distribution, ecological risk assessment and indicators screening, Mar. Pollut. Bull. 151 (2020), 110810, https://doi.org/10.1016/j.marpolbul.2019.110810.

[6] E.M.H. Wellington, A.B.A. Boxall, P. Cross, E.J. Feil, W.H. Gaze, P.M. Hawkey, A.S. Johnson-Rollings, D.L. Jones, N.M. Lee, W. Otten, C.M. Thomas, A. P. Williams, The role of the natural environment in the emergence of antibiotic resistance in Gram-negative bacteria, Lancet Infect. Dis. 13 (2) (2013) 155–165, https://doi.org/10.1016/S1473-3099(12)70317-1.

[7] M. Zhuang, Y. Achmon, Y. Cao, X. Liang, L. Chen, H. Wang, B.A. Siame, K.Y. Leung, Distribution of antibiotic resistance genes in the environment, Environ. Pollut. 285 (2021), 117402, https://doi.org/10.1016/j.envpol.2021.117402.

[8] N. Janecko, L. Pokludova, J. Blahova, Z. Svobodova, I. Literak, Implications of fluoroquinolone contamination for the aquatic environment-A review, Environ. Toxicol. Chem. 35 (11) (2016) 2647–2656, https://doi.org/10.1002/etc.3552.

[9] K. Wang, T. Zhuang, Z. Su, M. Chi, H. Wang, Antibiotic residues in wastewaters from sewage treatment plants and pharmaceutical industries: occurrence, removal and environmental impacts, Sci. Total Environ. 788 (2021), 147811, https://doi.org/10.1016/j.scitotenv.2021.147811.

[10] K. Kümmerer, Pharmaceuticals in the environment – a brief summary, in: K. Kümmerer (Ed.), Pharmaceuticals in the Environment: Sources, Fate, Effects and Risks, Springer Berlin Heidelberg, Berlin, Heidelberg, 2008, pp. 3–21, https://doi.org/10.1007/978-3-540-74664-5_1.

[11] C. Yan, M. Nie, Y. Yang, J. Zhou, M. Liu, M. Baalousha, J.R. Lead, Effect of colloids on the occurrence, distribution and photolysis of emerging organic contaminants in wastewaters, J. Hazard Mater. 299 (2015) 241–248, https://doi.org/10.1016/j.jhazmat.2015.06.022.

[12] S. Majumder, B. Nath, S. Sarkar, D. Chatterjee, G. Roman-Ross, M. Hidalgo, Size-fractionation of groundwater arsenic in alluvial aquifers of West Bengal, India: the role of organic and inorganic colloids, Sci. Total Environ. 468–469 (2014) 804–812, https://doi.org/10.1016/j.scitotenv.2013.08.087.

[13] M.F. Zaranyika, P. Dzomba, J. Kugara, Degradation of oxytetracycline in the aquatic environment: a proposed steady state kinetic model that takes into account hydrolysis, photolysis, microbial degradation and adsorption by colloidal and sediment particles, Environ. Chem. 12 (2) (2015) 174–188, https://doi.org/10.1071/EN14116.

[14] D. Cheng, X. Liu, S. Zhao, B. Cui, J. Bai, Z. Li, Influence of the natural colloids on the multi-phase distributions of antibiotics in the surface water from the largest lake in North China, Sci. Total Environ. 578 (2017) 649–659, https://doi.org/10.1016/j.scitotenv.2016.11.012.

[15] J. Li, H. Zhang, Adsorption-desorption of oxytetracycline on marine sediments: kinetics and influencing factors, Chemosphere 164 (2016) 156–163, https://doi.org/10.1016/j.chemosphere.2016.08.100.

[16] M. Pan, L.M. Chu, Adsorption and degradation of five selected antibiotics in agricultural soil, Sci. Total Environ. 545–546 (2016) 48–56, https://doi.org/10.1016/j.scitotenv.2015.12.040.

[17] J.R. Lead, K.J. Wilkinson, Aquatic colloids and nanoparticles: current knowledge and future trends, Environ. Chem. 3 (3) (2006) 159–171, https://doi.org/10.1071/EN06025.

[18] R.M. Briones, A.K. Sarmah, Insight into the sorption mechanism of metformin and its transformation product guanylurea in pastoral soils and model sorbents, Sci. Total Environ. 645 (2018) 1323–1333, https://doi.org/10.1016/j.scitotenv.2018.07.251.

[19] G. Liu, J. Wang, W. Xue, J. Zhao, J. Wang, X. Liu, Effect of the size of variable charge soil particles on cadmium accumulation and adsorption, J. Soils Sediments 17 (2017) 2810–2821, https://doi.org/10.1007/s11368-017-1712-6.

[20] K. Maskaoui, J.L. Zhou, Colloids as a sink for certain pharmaceuticals in the aquatic environment, Environ. Sci. Pollut. Res. 17 (4) (2010) 898–907, https://doi.org/10.1007/s11356-009-0279-1.

[21] Y. Yang, J. Fu, H. Peng, L. Hou, M. Liu, J.L. Zhou, Occurrence and phase distribution of selected pharmaceuticals in the Yangtze Estuary and its coastal zone, J. Hazard Mater. 190 (1–3) (2011) 588–596, https://doi.org/10.1016/j.jhazmat.2011.03.092.

[22] P.K. Mutiyar, A.K. Mittal, Occurrences and fate of selected human antibiotics in influents and effluents of sewage treatment plant and effluent-receiving river Yamuna in Delhi (India), Environ. Monit. Assess. 186 (2014) 541–557, https://doi.org/10.1007/s10661-013-3398-6.

[23] C. Yan, Y. Yang, J. Zhou, M. Nie, M. Liu, M.F. Hochella, Selected emerging organic contaminants in the Yangtze Estuary, China: a comprehensive treatment of their association with aquatic colloids, J. Hazard Mater. 283 (2015) 14–23, https://doi.org/10.1016/j.jhazmat.2014.09.011.

[24] S. Ji, X. Li, X. Meng, S. Xu, Q. Lin, Coupled effect of pH and kaolinite colloids on antibiotic transport in porous media, Pedosphere (2023), https://doi.org/10.1016/j.pedsph.2023.01.003.

[25] M. Wang, Q. Zhang, T. Lu, J. Chen, Q. Wei, W. Chen, Y. Zhou, Z. Qi, Colloid-mediated transport of tetracycline in saturated porous media: comparison between ferrihydrite and montmorillonite, J. Environ. Manag. 299 (2021) (2021), 113638, https://doi.org/10.1016/j.jenvman.2021.113638.

[26] J.D. Hu, Y. Zevi, X. Kou, J. Xiao, X. Wang, Y. Jin, Effect of dissolved organic matter on the stability of magnetite nanoparticles under different pH and ionic strength conditions, Sci. Total Environ. 408 (2010) 3477–3489, https://doi.org/10.1016/j.scitotenv.2010.03.033.

[27] W. Gong, X. Liu, H. He, L. Wang, G. Dai, Quantitatively modeling soil–water distribution coefficients of three antibiotics using soil physicochemical properties, Chemosphere 89 (7) (2012) 825–831, https://doi.org/10.1016/j.chemosphere.2012.04.064.

[28] B. Chu, K.W. Goyne, S.H. Anderson, C.H. Lin, R.N. Lerch, Sulfamethazine sorption to soil: vegetative management, pH, and dissolved organic matter effects, J. Environ. Qual. 42 (3) (2013) 794–805, https://doi.org/10.2134/jeq2012.0222.

[29] S.R. Wegst-Uhrich, D.A.G. Navarro, L. Zimmerman, D.S. Aga, Assessing antibiotic sorption in soil: a literature review and new case studies on sulfonamides and macrolides, Chem. Cent. J. 8 (5) (2014) 1–12, https://doi.org/10.1186/1752-153X-8-5.

[30] R. Beckett, N.P. Le, The role or organic matter and ionic composition in determining the surface charge of suspended particles in natural waters, Colloid. Surface. 44 (1990) 35–49, https://doi.org/10.1016/0166-6622(90)80185-7.

[31] A.J. Carrasquillo, G.L. Bruland, A.A. MacKay, D. Vasudevan, Sorption of ciprofloxacin and oxytetracycline zwitterions to soils and soil minerals: influence of compound structure, Environ. Sci. Technol. 42 (20) (2008) 7634–7642, https://doi.org/10.1021/es801277y.

[32] O. Lorphensri, J. Intravijit, D.A. Sabatini, T.C.G. Kibbey, K. Osathaphan, C. Saiwan, Sorption of acetaminophen, 17$\alpha$-ethynyl estradiol, nalidixic acid, and norfloxacin to silica, alumina, and a hydrophobic medium, Water Res. 40 (7) (2006) 1481–1491, https://doi.org/10.1016/j.watres.2006.02.003.

[33] X. Tong, Y. Li, F. Zhang, X. Chen, Y. Zhao, B. Hu, X. Zhang, Adsorption of 17$\beta$-estradiol onto humic-mineral complexes and effects of temperature, pH, and bisphenol A on the adsorption process, Environ. Pollut. 254 (2019), 112924, https://doi.org/10.1016/j.envpol.2019.07.092.

[34] A.D. Jones, G.L. Bruland, S.G. Agrawal, D. Vasudevan, Factors influencing the sorption of oxytetracycline to soils, Environ. Toxicol. Chem. 24 (4) (2005) 761–770, https://doi.org/10.1897/04-037R.1.

[35] Y. Zhao, J. Geng, X. Wang, X. Gu, S. Gao, Tetracycline adsorption on kaolinite: pH, metal cations and humic acid effects, Ecotoxicology 20 (2011) 1141–1147, https://doi.org/10.1007/s10646-011-0665-6.

[36] A.M. Shaker, Z.R. Komy, S.E.M. Heggy, M.E.A. El-Sayed, Kinetic study for adsorption humic acid on soil minerals, J. Phys. Chem. A 116 (45) (2012) 10889–10896, https://doi.org/10.1021/jp3078826.

[37] X. Huang, C. Yan, M. Nie, J. Chen, M. Ding, Effect of colloidal fluorescence properties on the complexation of chloramphenicol and carbamazepine to the natural aquatic colloids, Chemosphere 286 (2022), 131604, https://doi.org/10.1016/j.chemosphere.2021.131604.

[38] Y. Wang, L. Zhong, X. Song, M. Adeel, Y. Yang, Natural colloids facilitated transport of steroidal estrogens in saturated porous media: mechanism and processes, Environ. Pollut. 315 (2022), 120315, https://doi.org/10.1016/j.envpol.2022.120315.

[39] H.A. Duong, N.H. Pham, H.T. Nguyen, T.T. Hoang, H.V. Pham, V.C. Pham, M. Berg, W. Giger, A.C. Alder, Occurrence, fate and antibiotic resistance of fluoroquinolone antibacterials in hospital wastewaters in Hanoi, Vietnam, Chemosphere 72 (6) (2008) 968–973, https://doi.org/10.1016/j.chemosphere.2008.03.009.

[40] X. Zhu, J. He, S. Su, X. Zhang, F. Wang, Concept model of the formation process of humic acid–kaolin complexes deduced by trichloroethylene sorption experiments and various characterizations, Chemosphere 151 (2016) 116–123, https://doi.org/10.1016/j.chemosphere.2016.02.068.

[41] D. Cheng, H. Liu, Y. E, F. Liu, H. Lin, X. Liu, Effects of natural colloidal particles derived from a shallow lake on the photodegradation of ofloxacin and ciprofloxacin, Sci. Total Environ. 773 (2021), 145102, https://doi.org/10.1016/j.scitotenv.2021.145102.

[42] I. Langmuir, The adsorption of gases on plane surfaces of glass, mica and platinum, J. Am. Chem. Soc. 40 (9) (1918) 1361–1403, https://doi.org/10.1021/ja02242a004.

[43] Y. Luo, J. Chen, C. Wu, J. Zhang, J. Tang, J. Shang, Q. Liao, Effect of particle size on adsorption of norfloxacin and tetracycline onto suspended particulate matter in lake, Environ. Pollut. 244 (2019) 549–559, https://doi.org/10.1016/j.envpol.2018.10.066.

[44] D. Hank, Z. Azi, S. Ait Hocine, O. Chaalal, A. Hellal, Optimization of phenol adsorption onto bentonite by factorial design methodology, J. Ind. Eng. Chem. 20 (4) (2014) 2256–2263, https://doi.org/10.1016/j.jiec.2013.09.058.

[45] R.P. Schwarzenbach, P.M. Gschwend, D.M. Imboden, Sorption I: general introduction and sorption processes involving oganic matter, in: Environmental Organic Chemistry, John Wiley & Sons, Inc., Hoboken, New Jersey, Canada, 2002, pp. 275–330, https://doi.org/10.1002/0471649643.ch9.

[46] Y. Zhu, Q. Yang, T. Lu, W. Qi, H. Zhang, M. Wang, Z. Qi, W. Chen, Effect of phosphate on the adsorption of antibiotics onto iron oxide minerals: comparison between tetracycline and ciprofloxacin, Ecotoxicol. Environ. Saf. 205 (2020), 111345, https://doi.org/10.1016/j.ecoenv.2020.111345.

[47] Y. Yu, X. Liu, W. Cong, G. Liu, D. Cheng, H. Bao, D. Gao, Adsorption of potentially toxic metals on negatively charged liposomes: equilibrium isotherms and quantitative modeling, RSC Adv. 4 (2014) 42591–42597, https://doi.org/10.1039/C4RA04775C.

[48] F. Kallel, F. Chaari, F. Bouaziz, F. Bettaieb, R. Ghorbel, S.E. Chaabouni, Sorption and desorption characteristics for the removal of a toxic dye, methylene blue from aqueous solution by a low cost agricultural by-product, J. Mol. Liq. 219 (2016) 279–288, https://doi.org/10.1016/j.molliq.2016.03.024.

[49] M. Mobarak, A.Q. Selim, E.A. Mohamed, M.K. Seliem, A superior adsorbent of CTAB/$H_2O_2$ solution−modified organic carbon rich-clay for hexavalent chromium and methyl orange uptake from solutions, J. Mol. Liq. 259 (2018) 384–397, https://doi.org/10.1016/j.molliq.2018.02.014.

[50] S.M. Al-Jubouri, H.A. Al-Jendeel, S.A. Rashid, S. Al-Batty, Antibiotics adsorption from contaminated water by composites of ZSM-5 zeolite nanocrystals coated carbon, J. Water Process Eng. 47 (2022), 102745, https://doi.org/10.1016/j.jwpe.2022.102745.

[51] S.T. Danalıoğlu, Ş.S. Bayazit, Ö. Kerkez, B.G. Alhogbi, M. Abdel Salam, Removal of ciprofloxacin from aqueous solution using humic acid- and levulinic acid-coated $Fe_3O_4$ nanoparticles, Chem. Eng. Res. Des. 123 (2017) 259–267, https://doi.org/10.1016/j.cherd.2017.05.018.

[52] J. Zhou, F. Ma, H. Guo, Adsorption behavior of tetracycline from aqueous solution on ferroferric oxide nanoparticles assisted powdered activated carbon, Chem. Eng. J. 384 (2020), 123290, https://doi.org/10.1016/j.cej.2019.123290.

[53] S. Chen, C. Qin, T. Wang, F. Chen, X. Li, H. Hou, M. Zhou, Study on the adsorption of dyestuffs with different properties by sludge-rice husk biochar: adsorption capacity, isotherm, kinetic, thermodynamics and mechanism, J. Mol. Liq. 285 (2019) 62–74, https://doi.org/10.1016/j.molliq.2019.04.035.

[54] W. Feng, A.F. Plante, A.K. Aufdenkampe, J. Six, Soil organic matter stability in organo-mineral complexes as a function of increasing C loading, Soil Boil. Biochem. 69 (2014) 398–405, https://doi.org/10.1016/j.soilbio.2013.11.024.

[55] C.N. Duong, J.S. Ra, D. Schlenk, S.D. Kim, H.K. Choi, S.D. Kim, Sorption of estrogens onto different fractions of sediment and its effect on vitellogenin expression in Male Japanese Medaka, Arch. Environ. Contam. Toxicol. 59 (2010) 147–156, https://doi.org/10.1007/s00244-009-9429-1.

[56] Y. Luo, J. Chen, C. Wu, J. Zhang, J. Tang, J. Shang, Q. Liao, Effect of particle size on adsorption of norfloxacin and tetracycline onto suspended particulate matter in lake, Environ. Pollut. 244 (2019) 549–559, https://doi.org/10.1016/j.envpol.2018.10.066.

[57] Q. Mo, X. Yang, J. Wang, H. Xu, W. Li, Q. Fan, S. Gao, W. Yang, C. Gao, D. Liao, Y. Li, Y. Zhang, Adsorption mechanism of two pesticides on polyethylene and polypropylene microplastics: DFT calculations and particle size effects, Environ. Pollut. 291 (2021), 118120, https://doi.org/10.1016/j.envpol.2021.118120.

[58] Q. Yang, X. Li, G. Chen, J. Zhang, B. Xing, Effect of humic acid on the sulfamethazine adsorption by functionalized multi-walled carbon nanotubes in aqueous solution: mechanistic study, RSC Adv. 6 (2016) 15184–15191, https://doi.org/10.1039/C5RA26913J.

[59] Z. Zhang, Q. Gao, Z. Xie, J. Yang, J. Liu, Adsorption of nitrification inhibitor nitrapyrin by humic acid and fulvic acid in black soil: characteristics and mechanism, RSC Adv. 11 (2021) 114–123, https://doi.org/10.1039/D0RA08714A.

[60] J.N. Uwayezu, L.W.Y. Yeung, M. Bäckström, Sorption of PFOS isomers on goethite as a function of pH, dissolved organic matter (humic and fulvic acid) and sulfate, Chemosphere 233 (2019) 896–904, https://doi.org/10.1016/j.chemosphere.2019.05.252.

[61] G.R. Aiken, H. Hsu-Kim, J.N. Ryan, Influence of dissolved organic matter on the environmental fate of metals, nanoparticles, and colloids, Environ. Sci. Technol. 45 (8) (2011) 3196–3201, https://doi.org/10.1021/es103992s.

[62] A. Philippe, G.E. Schaumann, Interactions of dissolved organic matter with natural and engineered inorganic colloids: a review, Environ. Sci. Technol. 48 (16) (2014) 8946–8962, https://doi.org/10.1021/es502342r.

[63] S. Sachs, G. Bernhard, Sorption of U(VI) onto an artificial humic substance-kaolinite-associate, Chemosphere 72 (10) (2008) 1441–1447, https://doi.org/10.1016/j.chemosphere.2008.05.027.

[64] A. Li, M. Xu, W. Li, X. Wang, J. Dai, Adsorption characterizations of fulvic acid fractions onto kaolinite, J. Environ. Sci. 20 (5) (2008) 528–535, https://doi.org/10.1016/S1001-0742(08)62090-2.

[65] L. Zhang, L. Luo, S. Zhang, Integrated investigations on the adsorption mechanisms of fulvic and humic acids on three clay minerals, Colloid. Surface. 406 (2012) 84–90, https://doi.org/10.1016/j.colsurfa.2012.05.003.

[66] Y. Wang, W. Yu, Z. Chang, C. Gao, Y. Yang, B. Zhang, Y. Wang, B. Xing, Effects of dissolved organic matter on the adsorption of norfloxacin on a sandy soil (fraction) from the Yellow River of Northern China, Sci. Total Environ. 848 (2022), 157495, https://doi.org/10.1016/j.scitotenv.2022.157495.

[67] A.A. Ahmed, S. Thiele-Bruhn, S.G. Aziz, R.H. Hilal, S.A. Elroby, A.O. Al-Youbi, P. Leinweber, O. Kühn, Interaction of polar and nonpolar organic pollutants with soil organic matter: sorption experiments and molecular dynamics simulation, Sci. Total Environ. 508 (2015) 276–287, https://doi.org/10.1016/j.scitotenv.2014.11.087.

[68] L. Liang, L. Luo, S. Zhang, Adsorption and desorption of humic and fulvic acids on $SiO_2$ particles at nano- and micro-scales, Colloid. Surface. 384 (1–3) (2011) 126–130, https://doi.org/10.1016/j.colsurfa.2011.03.045.

[69] M. Kastelan-Macan, M. Petrovic, The role of fulvic acids in phosphorus sorption and release from mineral particles, Water Sci. Technol. 34 (7–8) (1996) 259–265, https://doi.org/10.1016/S0273-1223(96)00753-6.

[70] M. Sillanpää, A. Matilainen, T. Lahtinen, Chapter 2 - characterization of NOM, in: M. Sillanpää (Ed.), Natural Organic Matter in Water, Butterworth-Heinemann, 2015, pp. 17–53, https://doi.org/10.1016/B978-0-12-801503-2.00002-1.

[71] V. Artifon, E. Zanardi-Lamardo, G. Fillmann, Aquatic organic matter: classification and interaction with organic microcontaminants, Sci. Total Environ. 649 (2019) 1620–1635, https://doi.org/10.1016/j.scitotenv.2018.08.385.

[72] R.M.P. Leal, L.R.F. Alleoni, V.L. Tornisielo, J.B. Regitano, Sorption of fluoroquinolones and sulfonamides in 13 Brazilian soils, Chemosphere 92 (8) (2013) 979–985, https://doi.org/10.1016/j.chemosphere.2013.03.018.

[73] Y. Wan, X. Liu, P. Liu, L. Zhao, W. Zou, Optimization adsorption of norfloxacin onto polydopamine microspheres from aqueous solution: kinetic, equilibrium and adsorption mechanism studies, Sci. Total Environ. 639 (2018) 428–437, https://doi.org/10.1016/j.scitotenv.2018.05.171.

[74] L. Zhao, J. Liu, H. Wang, Y. Dong, Sorption of copper and norfloxacin onto humic acid: effects of pH, ionic strength, and foreign ions, Environ. Sci. Pollut. Res. 26 (11) (2019) 10685–10694, https://doi.org/10.1007/s11356-019-04515-5.

[75] W. Sun, K. Yin, X. Yu, Effect of natural aquatic colloids on Cu(II) and Pb(II) adsorption by $Al_2O_3$ nanoparticles, Chem. Eng. J. 225 (2013) 464–473, https://doi.org/10.1016/j.cej.2013.04.010.

[76] T. Yang, N. Wang, H. Gu, The adsorption behavior of niobium (V) on kaolin clay and kaolinite, Appl. Clay Sci. 235 (2023), 106866, https://doi.org/10.1016/j.clay.2023.106866.
[77] H. Du, J. Du, F. Liu, Y. Zhang, H. Guo, D. Wan, Binding of tetracycline on soil phyllosilicates with Cd(II) as affected by pH and mineral type, J. Soils Sediments 21 (2021) 775–783, https://doi.org/10.1007/s11368-020-02867-x.
[78] Z. Zhang, K. Sun, B. Gao, G. Zhang, X. Liu, Y. Zhao, Adsorption of tetracycline on soil and sediment: effects of pH and the presence of Cu(II), J. Hazard Mater. 190 (1–3) (2011) 856–862, https://doi.org/10.1016/j.jhazmat.2011.04.017.
[79] S.D. Sibley, J.A. Pedersen, Interaction of the macrolide antimicrobial clarithromycin with dissolved humic acid, Environ. Sci. Technol. 42 (2) (2008) 422–428, https://doi.org/10.1021/es071467d.
[80] S.A. Sassman, L.S. Lee, Sorption of three tetracyclines by several soils: assessing the role of pH and cation exchange, Environ. Sci. Technol. 39 (19) (2005) 7452–7459, https://doi.org/10.1021/es0480217.
[81] H.T. Nguyen, V.N. Phuong, T.N. Van, P.N. Thi, P. Dinh Thi Lan, H.T. Pham, H.T. Cao, Low-cost hydrogel derived from agro-waste for veterinary antibiotic removal: optimization, kinetics, and toxicity evaluation, Environ. Technol. Innov. 20 (2020), 101098, https://doi.org/10.1016/j.eti.2020.101098.
[82] H. Zhang, S. Xu, Q. Lin, Influence of metal cation and surface iron oxide on the transport of sulfadiazine in saturated porous media, Sci. Total Environ. 758 (2021), 143621, https://doi.org/10.1016/j.scitotenv.2020.143621.
[83] A. Takdastan, A.H. Mahvi, E.C. Lima, M. Shirmardi, A.A. Babaei, G. Goudarzi, A. Neisi, M. Heidari Farsani, M. Vosoughi, Preparation, characterization, and application of activated carbon from low-cost material for the adsorption of tetracycline antibiotic from aqueous solutions, Water Sci. Technol. 74 (10) (2016) 2349–2363, https://doi.org/10.2166/wst.2016.402.
[84] Y. Zhao, J. Geng, X. Wang, X. Gu, S. Gao, Adsorption of tetracycline onto goethite in the presence of metal cations and humic substances, J. Colloid Interface Sci. 361 (1) (2011) 247–251, https://doi.org/10.1016/j.jcis.2011.05.051.
[85] Y. Xu, X. Yu, B. Xu, D. Peng, X. Guo, Sorption of pharmaceuticals and personal care products on soil and soil components: influencing factors and mechanisms, Sci. Total Environ. 753 (2021), 141891, https://doi.org/10.1016/j.scitotenv.2020.141891.
[86] Y. Li, S. Wang, Y. Zhang, R. Han, W. Wei, Enhanced tetracycline adsorption onto hydroxyapatite by Fe(III) incorporation, J. Mol. Liq. 247 (2017) 171–181, https://doi.org/10.1016/j.molliq.2017.09.110.